TRACE ELEMENTAL ABUNDANCES IN CALCIUM-ALUMINUM-RICH INCLUSIONS IN CV CHONDRITES X. Mouti Al-Hashimi[1,2], P. Mane[1], J.B. Setera[3], J.I. Simon[4], [1]Lunar and Planetary Institute, Universities Space Research Association, Houston, TX 77058, [2]Arizona State University, Tempe, AZ 85281 (xmouti@asu.edu), [3]University of Texas at El Paso/Jacobs-JETS, NASA Johnson Space Center, Houston, TX 77058, [4]Center for Isotope Cosmochemistry & Geochronology, NASA Johnson Space Center, Houston, TX 77058.

Introduction: Calcium-aluminum-rich inclusions (CAIs), are the first formed solids that define the age of the Solar System [1,2]. CAIs are thought to have condensed from nebular gas [3,4] within the first <1 Ma of Solar System formation [5,6]. CAIs have experienced numerous early Solar System processes including condensation, evaporation, melting, recrystallization, and aqueous alteration [e.g., 7]. The chemical, mineralogical, and textural diversity among CAIs results from a range of chemical and physical processes recorded in nebular and parent body settings. This study explores the mineralogical, textural, and chemical compositions of CAIs including the trace elemental abundances in CAI phases to determine the early Solar System processes recorded in them.

Samples and Analytical Methods: We analyzed one CAI each from CV3 chondrites Northwest Africa (NWA) 5508 designated as 'Saguaro', and Northwest Africa (NWA) 12772 designated as 'Hoopoe'. Back-scatter electron (BSE) images were collected using a Phenom XL scanning electron microscope (SEM) at the Lunar and Planetary Institute (LPI) and the JEOL JXA-8530F electron probe microanalyzer (EPMA) at Johnson Space Center (JSC)-NASA. Additionally, energy dispersive X-ray spectrometry (EDS) elemental maps of select areas for these samples were collected using a 15.0kV beam energy and a 40µA emission current. Using the EPMA, wavelength-dispersive X-ray spectrometry (WDS) quantitative major elemental abundances were determined. *In-situ* trace element measurements for both CAIs were performed at JSC-NASA using a Photon Machines 193nm laser ablation system and a Thermo-Scientific Element-XR inductively coupled plasma mass spectrometer (ICP-MS). Analyses consisted of 30s ablations at 10Hz, spot sizes of 20-25µm, and a fluence of 6.0 J/cm^2 for anorthite and melilite, and a 3.5 J/cm^2 fluence for all other phases. NIST612 was used to correct for instrument drift, while BHVO-2g was used as a primary calibration standard. BCR-2g and in-house mineral standards were regularly measured as unknowns to ensure accuracy.

Results and Discussion: Saguaro is a coarse-grained CAI, ~11 x 6 mm in dimensions. Saguaro contains spinel, Al-rich pyroxene, anorthite, Mg-rich melilite, and minor perovskite in its interior and is therefore classified as a Type B CAI. Åk content of melilite in Saguaro ranges from ~24 to 54 with no apparent trend from the core to the edge of the CAI. The spinel appears euhedral and occurs both as clusters and as spinel palisades [8]. The presence of spinel palisades in Saguaro suggests that it experienced melting and recrystallization [9]. Two rim sequences surround most of the inclusion: the inner Wark-Lovering (WL) rim sequence (~10-35 µm) containing pyroxene, spinel, and melilite (+ anorthite), and the outer rim sequence is a finer-grained, thicker accretionary rim (Fig. 1).

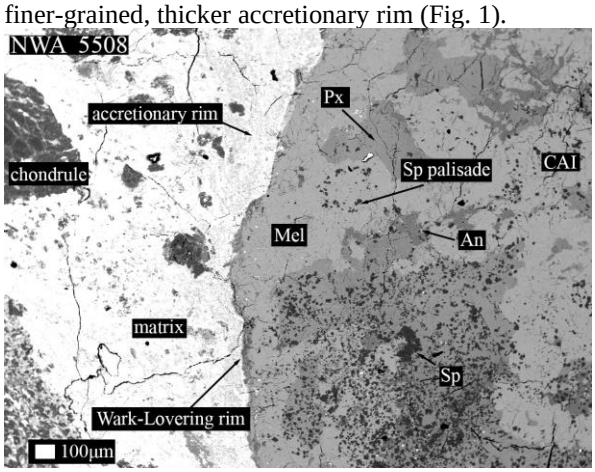

Figure 1. BSE image from NWA 5508 showing CAI Saguaro.

The mineral phases in Saguaro record an overall flat REE pattern with an average negative Eu anomaly in pyroxene, and an average positive Eu anomaly in anorthite and melilite. Anorthite, melilite, and pyroxene show depletion in Tm (Fig. 2).

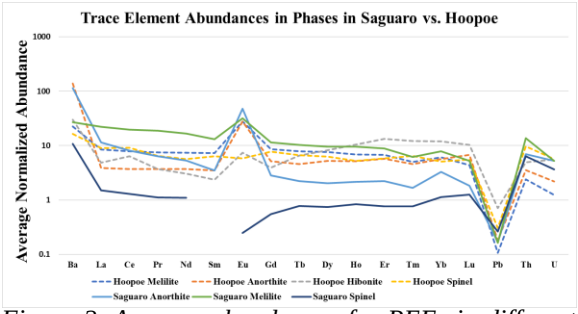

Figure 2. Average abundances for REEs in different phases in Hoopoe and Saguaro. Abundances normalized to the values for CI chondrites [10].

The Hoopoe CAI is compact, coarse-grained and ~6 × 4 mm in size. The major mineralogy includes hibonite, spinel, melilite, anorthite, and perovskite. Therefore, it can be interpreted as a compact transitional type A and B. Hibonite in Hoopoe shows

variations in Al_2O_3 from 79 to 91 wt% and TiO_2 from 0.04 to 7.6 wt%. Hibonite appears to be pseudomorphically replacing the spinel, (i.e., is hibonite in composition, but appears in the shape of spinel). Individual melilite grains show compositional variations, where the Åk content of ranges from ~6 to 28. Melilite exhibits both homogenous and fractured textures. Spinel often appears clustered.

The WL-rim sequence surrounding Hoopoe is ~25 μm thick and composed of spinel, perovskite, hibonite, and melilite. It is then partially surrounded by an outer accretionary rim sequence (~75μm). Metal assemblages rich in Fe and Ni were observed in Hoopoe. All major mineral phases in Hoopoe display relatively flat REE patterns, except for varying Eu and Tm anomalies between phases (Fig. 2, 3). There is a prominent negative Eu anomaly in perovskite and an average positive Eu anomaly in spinel, anorthite, and hibonite respectively (Fig. 2, 3). The WL rim around Hoopoe also display a negative Eu anomaly.

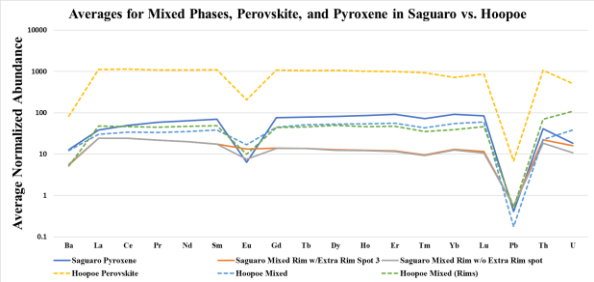

Figure 3. Average normalized abundances for REEs in perovskite, pyroxene, mineral mixtures, and multi-phase rim analyses in Hoopoe and Saguaro. Abundances normalized to the values for CI chondrites [10].

Trace elemental abundances: Mineral phases in Saguaro and Hoopoe record similar trace element patterns, with both appearing generally flat, with anomalies in Eu and Tm (Figs. 2, 3). Melilite and anorthite display positive Eu anomalies in both CAIs. Similarly, hibonite in Hoopoe also records a positive Eu anomaly (Fig. 2). In contrast, pyroxene and perovskite in both Saguaro and Hoopoe record negative Eu anomalies. (Fig. 3). Given that Eu is volatile in reducing environments [12], this may indicate reducing conditions in the surrounding nebular gas at the time anorthite and melilite crystallized. As these CAIs continued to form, this gas as a result would become depleted in Eu. This also could be supported by the propensity of anorthite and melilite to incorporate Eu from their surroundings [13]. In Saguaro, melilite and anorthite (Eu enriched) often surround the pyroxene (Eu depleted) as they are crystallized. The proximity, abundance, and intergrown relationships between phases may suggest that Eu is being preferentially incorporated into some phases, preventing it from being incorporated into others.

Trace elemental analyses of the CAI rims will be evaluated in more detail, as they are complicated by their smaller grain-size and therefore, transient signal being composed of a mixture of mineral phases. Broadly, however, the patterns in the rims of both CAIs are comparable to each other, and to the mixed phase patterns in the core of Hoopoe (Fig. 3). Other studies have found that CAI rims contain higher abundances of REEs compared to the interior and are depleted in Ce and Yb, suggesting that some WL rims form as evaporation residues [14]. However, we did not observe such differences between the rim and the interior of the two CAIs discussed here. Given their similarity, the trace elemental analyses of the mixed interior (i.e. core) and rim phases could be interpreted as forming from similar, if not the same, reservoirs. The REE abundance between the rim and core of Hoopoe are also similar, indicating they may have formed from a gas of the same or similar composition.

Acknowledgments: We thank the ASU Center for Meteorite Studies for loaning samples used in this work and Tabb Prissel for his assistance with the analysis. Mouti Al-Hashimi thanks Sam Crossley and Cyrena Goodrich for their help with the LPI SEM training. This work was supported by the LPI Summer Intern Program in Planetary Science and the LPI Cooperative Agreement.

References: [1] Connelly J.N. (2012) *Science, 338,* 651-655. [2] MacPherson G. J. (2014) *Treatise on Geochem., 2,* 139-179. [3] Grossman L. (1972) *GCA, 36,* 597-619. [4] Ebel, D.S. (2006) *Meteorites and the Early Solar System II (D. S. Lauretta & H. Y. McSween, Eds.)* 253-277. [5] MacPherson G. J. (2012) *Earth Planet. Sci. Lett., 331-332,* 43-54. [6] MacPherson G.J. (2017) *GCA, 201,* 65-82. [7] Krot A.N. (1995) *Meteoritics & Planet. Sci., 30,* 748-775. [8] Wark and Lovering (1982) *GCA, 46,* 2595-2607. [9] Simon S. B. and Grossman L. (1997) *Meteoritics & Planet. Sci., 32,* 61-70. [10] Palme H. and Jones A. (2003) *Treatise on Geochemistry (H. D. Holland and K. K. Turekian Eds.), 1,* 41-61. [11] Grossman L. (1980) *Ann. Rev. Earth Planet. Sci., 8,* 559-608. [12] Floss C. et al. (1996) *GCA, 60,* 1975-1997. [13] Mason B. and Martin P. M. (1974) *Earth Planet. Sci. Lett., 22,* 141-144. [14] Wark B. and Boynton W. V. (2001) *Meteoritics & Planet. Sci., 36,* 1135-1166.